Sensor-Based Construction of a Retract-Like Structure for a Planar Rod Robot

Howie Choset, *Member, IEEE,* and Ji Yeong Lee

***Abstract*—Sensor-based planning for rod-shaped robots is necessary for the realistic deployment of noncircularly symmetric robots into unknown environments. Whereas circularly symmetric robots have two-dimensional Euclidean configuration spaces, planar rod robots posses three degrees-of-freedom, two for position and one for orientation, and hence have a three-dimensional configuration space, $SE(2)$. In this work, we define the rod hierarchical generalized Voronoi graph (rod-HGVG) which is a roadmap of the rod's configuration space. Prior work in Voronoi-based roadmaps use a retraction of the robot's free space to define the roadmap; here, we break a part the robot's free space into regions where fragments of the roadmap are defined and then connect the fragments. The primary advantage of the rod-HGVG is that it is defined in terms of workspace distance measurements, which makes it amenable to sensor-based planning. This paper also includes a numerical procedure that generates the rod-HGVG edge fragments using only information that is within line of sight of the rod robot. It is worth noting that this procedure does not require an explicit definition of configuration space, i.e., this procedure constructs a roadmap of rod configuration space without ever constructing the configuration space itself.**

***Index Terms*—Generalized Voronoi graph, retractions, rod-shaped robots, sensor-based motion planning, Voronoi diagrams.**

I. Introduction

SENSOR-BASED planning makes use of sensor information reflecting, at best, line-of-sight information of the environment, in contrast to classical planning, which assumes full knowledge of the environment prior to planning. This paper develops an exploration technique for rod-shaped robots which posses a three-dimensional (3-D) configuration space $SE(2)$. Conventional planners first construct the robot's configuration space and then perform planning in the configuration space. However, for sensor-based planning, this is not possible because the environment is not known *a priori* and hence the configuration space for the rod cannot be constructed. Hence, the robot must construct a representation of the configuration space without explicitly constructing the configuration space itself.

This paper presents a method to incrementally construct a geometric structure, termed a *roadmap*, that captures the salient geometric features of the rod's configuration space. Canny originally defined a roadmap as a one-dimensional subset of the free space that is connected within each connected component of the free space [1], [2]. All algorithms that use a roadmap assume that there exists a path between any point in the free space to the roadmap. A planner uses the roadmap by finding a path from both the start and the goal to the roadmap and then between their respective "accessed" points on the roadmap. If the start and goal lie in the same connected component of free space, then their respective accessed points lie on the same connected roadmap component. This is how roadmaps "capture the connectivity" of the free space [3].

Motivated by Rimon and Canny's work [4], we use a sensor-based definition of a roadmap. A roadmap is a one-dimensional network of curves that have the following important properties: *accessibility*, *connectivity* and *departability*. These properties imply that the planner can determine a path between any two points in a connected component of the robot's free space by first finding a path onto the roadmap (accessibility), traversing the roadmap to the vicinity of the goal (connectivity) and then constructing a path from the roadmap to the goal (departability). When full knowledge of the world is available, then departability can be viewed as accessibility, but in reverse. However, if *a priori* knowledge is not available, the planner must determine on-line when to depart the roadmap, as opposed to determining a path from the goal to the roadmap. If the planner can construct the roadmap using line-of-sight sensor information, then it has in essence explored the free space because the planner can use the roadmap to plan future excursions through the free space.

This paper defines a new roadmap for rod-shaped robots whose configuration space is $SE(2)$ and prescribes the incremental construction procedures to construct the roadmap, i.e., explore an unknown $SE(2)$ configuration space. Since exploration is more general than navigation, we will focus discussion on exploration in this paper. This new roadmap, termed rod hierarchical generalized Voronoi graph (rod-HGVG), is defined in terms of distance to workspace obstacles. This feature is important for sensor-based planning because we can use real sensory data to construct the rod-HGVG. In Section III, we demonstrate how to lift workspace distance into configuration space through the forward kinematic map. Computing the gradient (really the differential) of the distance in configuration space is nontrivial because we need to factor in orientation motion, as well as translational motion.

With the definition of distance and gradient in-hand, in Section IV, we then present the rod-generalized Voronoi graph (rod-GVG), whose definition was motivated by the generalized Voronoi graph (GVG) [5], a roadmap for a point operating in $\mathbb{R}^3$. Unfortunately, just like the point-GVG, the rod-GVG is not guaranteed to be connected in a connected component of free space and thus in Section VI we define additional structures resulting

Manuscript received September 8, 1999; revised December 11, 2000. This paper was recommended for publication by Associate Editor J-P. Laumond and Editor S. Salcudean upon evaluation of the reviewers' comments. This work was supported by the Office of Naval Research under Grant 97PR06977 and the National Science Foundation under Grant IRI-9702768. This paper was presented at the International Conference on Robotics and Automation, Minneapolis, MN, 1996.

The authors are with the Department of Mechanical Engineering, Carnegie Mellon University, Pittsburgh, PA 15213 USA (e-mail: choset@ri.cmu.edu).

Publisher Item Identifier S 1042-296X(01)08446-4.

in the rod-hierarchical generalized Voronoi graph (rod-HGVG) which is proven to be a roadmap of $SE(2)$ in Section VII. The major challenge here is to demonstrate connectivity of the roadmap in its configuration space. We demonstrate connectivity by dividing the free space into cells called junction regions where the rod-GVG edges serve as retracts of the junction regions and then we use the point-GVG to connect the retracts (i.e., the rod-GVG edges) of adjacent junction regions.

Finally, using numerical methods similar to those presented in [6], we present an incremental construction technique for the rod-HGVG. Essentially, these numerical continuation techniques trace the roots of an equation comprising workspace distance functions and thus this procedure only requires distance information that sensors provide. Once the rod-HGVG is constructed, then the rod robot has essentially explored its configuration space because it can use the rod-HGVG for future excursions into the configuration space. This paper presents one of the first formulations of an algorithm that explores an non-Euclidean configuration space.

II. Relation to Prior Work

Sensor-based planning has received increased attention, as it is a requirement for realistic deployment of autonomous robots in unstructured environments. For a review of many sensor-based planning techniques, see [7]. Unfortunately, current sensor-based planning methods are limited because: (1) many are based on heuristic algorithms and it is therefore impossible to prove if they will work in all possible environments; (2) proof of convergence for other algorithms is limited to the case of a point in two-dimensional environments (for example, Lumelsky's "bug" algorithm [8]); or (3) the configuration space is assumed to be Euclidean (or diffeomorphic to a Euclidean space), which does not accurately represent many robots, including rod-shaped ones, nor addresses the issues of inferring distance to configuration space obstacles using sensor data. The goal of this work is to develop provably correct rod motion planning schemes that can be robustly implemented with realistic sensors.

The results presented in this paper are based on two related areas of previous work: Voronoi diagrams[9] and incremental methods to construct geometric structures [6], [10]. The first line of research starts with the generalized Voronoi diagram (GVD), a roadmap that was first used for motion planning in [11]. Active research in applying Voronoi diagrams to motion planning began with Ó'Dúnlaing and Yap's work [12], which considered motion planning for a disk in the plane. Let us denote the GVD as the point-GVD to later distinguish it from its rod counterpart. The point-GVD is defined in terms of a distance function

$$d_i(r) = \min_{c \in C_i} \|r - c\|$$

where $r \in \mathbb{R}^2$ and C_i is a convex obstacle. The basic building block of the point-GVD is the two-equidistant surjective surface,[1] which is a set of points equidistant to two convex obstacles and is denoted

$$\mathcal{SS}_{ij} = \{r \in \mathbb{R}^m : (d_i - d_j)(r) = 0 \text{ and } \nabla d_i(r) \neq \nabla d_j(r)\}$$

[1]In $\mathbb{R}^2$, $\mathcal{SS}_{ij}$ is one-dimensional and thus should be called a *curve*, but in $\mathbb{R}^m$ for $m > 2$, $\mathcal{SS}_{ij}$ is a surface and since we will be using this as a surface later on, we will term $\mathcal{SS}_{ij}$ structures as surfaces.

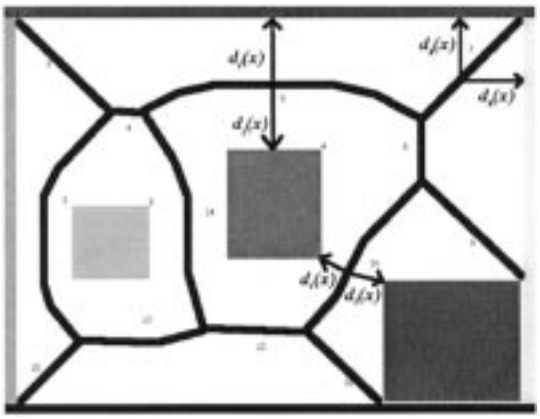

Fig. 1. Solid line segments correspond to the set of points equidistant to two obstacles, i.e., the point-GVD.

where $\nabla d_i(r)$ is a unit vector based at r, the closest point to C_i and pointing away from c along a line defined by c and r. In constructing the point-GVD, we are interested in a subset of $\mathcal{SS}_{ij}$ termed the two-equidistant face[2] which is defined as

$$\mathcal{F}_{ij} = \{r \in \text{cl}(\mathcal{SS}_{ij}) : d_i(r) \leq d_h(r)\ \forall h\}.$$

For an environment with n obstacles, the point-GVD is $\bigcup_{i=1}^{n-1} \bigcup_{j=i+1}^{n} \mathcal{F}_{ij}$. See Fig. 1.

Ó'Dúnlaing and Yap show that the point-GVD is a *retract* of the robot's free space. Recall that the retract is a set $A \subset X$ such that a continuous function $f : X \to A$ has $f(a) = a$ for all $a \in A$. In fact, the point-GVD is indeed a *strong deformation retract*, the image of a continuous function $f : X \to A$ that is homotopic to the identity map. Since any path in the robot's free space can be "retracted" onto the point-GVD, planar path planning between two points is achieved by planning a path onto the point-GVD, along the point-GVD and then to the goal.

One intuitive way of viewing the point-GVD is as the set of centers of circles that are tangent to two or more obstacles; since the set of points on a circle are equidistant to its center, when the circle "touches" the boundary of two or more obstacles, the center is at least two-way equidistance to nearby obstacles. Naturally, this circle is elastic and thus can extend and contract as its center moves along the point-GVD.

Choset and Burdick extended the point-GVD into higher dimensions by defining the generalized Voronoi graph (GVG). Whereas the point-GVD is equidistant to two obstacles in the plane, the point-GVG is equidistant to three obstacles in $\mathbb{R}^3$ (Fig. 2). Here, instead of looking at the centers of circles that touch two obstacles, consider the centers of spheres that are tangent to three or more obstacles; the centers of such spheres will be at least three-way equidistant. The point-GVG by itself is not connected, thus additional structures termed higher order Voronoi graphs are defined. The resulting roadmap is the point-hierarchical generalized Voronoi graph (point-HGVG).

The Voronoi diagram method in [12] was extended to the case where the robot is a rod in [13], but it requires full knowledge of the world's geometry prior to the planning event. Instead of

[2]We use the term surface to represent unbounded structures and faces to represent bounded ones.

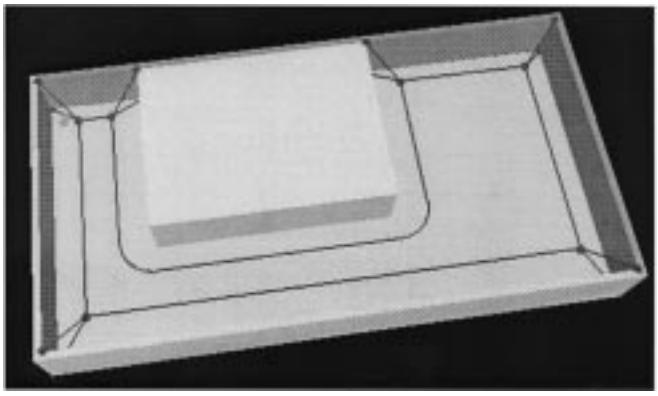

Fig. 2. The ceiling is removed from this rectangular enclosure that has a rectangular prism in its interior. The solid line segments correspond to the set of points equidistant to three obstacles, i.e., the point-GVG. Consider the "front-most" edge at the bottom of the figure. Imagine a sphere that touches the floor, front wall and ceiling (which is not displayed so we can see inside). The center of this sphere traces the point-GVG edge associated with these three obstacles. This center of this sphere can be used to trace the remaining point-GVG. Note that for the "spikes" in the corners of the workspace, the sphere contracts and expands.

looking at circle, the set of point equidistant to a point, Ó'Dúnlaing and Yap consider a *race-track*, the set of points equidistant to a rod [13]. They use the term race-track because the locus of points equidistant to a rod looks like a race-track; it has two straight edges parallel to the length of the rod and two semi-circular caps that go around the two end-points of the rod.

The set of rod configurations where the race-track is tangent to three or more obstacles forms a one-dimensional set in the rod's configuration space. This observation motivated our definition of the rod-GVG edge (see below) in that Ó'Dúnlaing and Yap did not have to resort to explicitly constructing a configuration space to define a structure in it. Our work rests upon this key result which we were then able to take two steps further. Although their race-track edge and our rod-GVG edge are the same, our first contribution is that we supply a method by which the rod-GVG can be constructed with on-line data. Our second contribution is that we developed a straight forward and sensor-based way to connect disconnected rod-GVG edges; the approach by Ó'Dúnlaing and Yap requires full knowledge of the environment.

Subsequently, Cox and Yap [14] developed an "on-line" strategy for path planning for rods. Although this method can be readily modified with tactile sensors for sensor-based use, it does not provide a roadmap of the rod robot's free space. The goal of the work described in this paper is to define a roadmap for a rod in its configuration space and demonstrate that it can be constructed using realistic sensors. Finally, Yap develops a cellular decomposition for rod path planning where each cell is defined in terms of critical points of rod-contact function [15]. Takahashi and Schilling [16] develop heuristic approaches that lifts the point-GVD into configuration space for a rectangularly shaped robot. Their heuristics for rectangular robots bare similarities to the approach we present for a rod robot, which can be viewed as a degenerate rectangle of zero width. For example, they position the rectangle to be "tangent" to the point-GVD much in the same way we form R-edges.

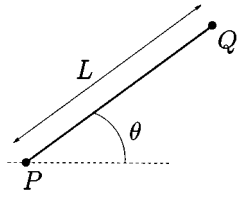

Fig. 3. The configuration of a rod is determined by the x and y coordinates of P and the orientation of the rod with respect to the horizontal.

The second line of research started with an incremental approach to creating a Voronoi diagram-like structure, which is limited to circular robots in the plane [17]. To our knowledge, the only endeavors pertaining to sensor-based adaptations of roadmaps for configuration space dimensions greater than two are Rimon and Canny's extension [4] of the Opportunistic Path Planner method [2] and Choset and Burdick's incremental construction procedure for the point-GVD and point-HGVG [5], [18].

A limitation of these roadmaps is that distance measurements are assumed to be made in a configuration space (or some parameterization of it). This assumption is reasonable for configuration spaces that are Euclidean, but extra care must be taken for non-Euclidean configuration spaces. Latombe [3] addresses this problem for potential functions defined in non-Euclidean spaces by considering a set of control points on the robot and then summing the potential function for each control point. He then applies the chain rule on the distance function and forward kinematic map to determine a true gradient in the non-Euclidean space. The first contribution of this paper uses a similar method to derive the gradient of a distance function in a non-Euclidean space.

III. Rod Distance Function

Definition 1: A **rod** R is a line segment of length L that has two end points P and Q.

The configuration space of the rod is $SE(2)$ ($SE(2) \simeq \mathbb{R}^2 \times S^1$). Let q be the configuration of the rod and let it be determined by the x and y coordinates of the point P and the orientation of the rod with respect to the horizontal, i.e., $q = (x, y, \theta)^T$ (Fig. 3). For $q \in SE(2)$, let $P(q)$ be the x and y coordinates of the point P, let $\theta(q)$ be the orientation of the rod and let $R(q)$ be the set of points in the plane that the rod occupies. When the rod achieves configuration q. Note that $P(q) \in \mathbb{R}^2$, $\theta(q) \in S^1$ and $R(q) \subset \mathbb{R}^2$. Let superscripts ^{x} and ^{y} denote the x and y coordinates, respectively, of a point in the plane. For example, $P(q)^x$ is the x coordinate of the point P at configuration q.

Assume a rod robot R is operating in a subset $\mathcal{W}$ of $\mathbb{R}^2$. $\mathcal{W}$ is populated by obstacles $C_1, \ldots, C_n$ which are convex sets. Non-convex obstacles are modeled as the union of convex shapes. It is assumed that the boundary of $\mathcal{W}$ is a collection of convex sets, which are members of the obstacle set $\{C_i\}$.

Definition 2: (Rod Single Object Distance) The rod single object distance function is the distance between an obstacle C_i and a rod R when the rod is at a configuration q. It is determined by

$$D_i(q) = \min_{r \in R(q), c \in C_i} \|r - c\|. \tag{1}$$

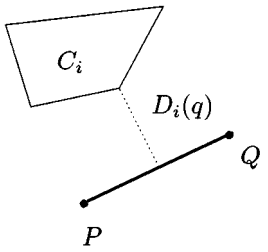

Fig. 4. The distance from the rod (thick solid line) to an obstacle is the distance (dotted line) between the nearest point on the rod to the obstacle and the nearest point on the obstacle to the rod.

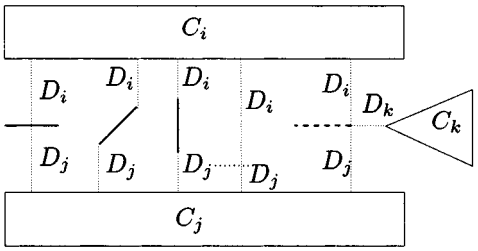

Fig. 5. The thick solid lines are rods which are in the configuration two-equidistant face defined by obstacles C_i and C_j. The light dotted lines delineate the distance to the nearest obstacle. The thick dotted line is an example of a rod which is not in a configuration two-equidistant face because it is closer to C_j than C_i. The thick dashed line is not in the two-equidistant face either because it is closer to C_k.

An important characteristic of $D_i(q)$ is that it can be readily computed from sensor measurements made in the workspace. For example, the rod robot in Fig. 4 may have range sensors distributed around its perimeter. The distance between the obstacle and the rod is the measurement of the range sensor associated with a local minima of measurements.

It can be shown that the rod-distance function is continuous and smooth in the interior of the workspace for convex sets. The multi-object rod-distance function, $D(q) = \min_i D_i(q)$, is also continuous but not smooth (even for convex obstacles).

IV. Rod-GVG: Building Block of the Rod-HGVG

Using work space distance information, we can now define the roadmap structure for the planar rod in its configuration space, $SE(2)$. The rod roadmap is defined in three steps: first, we define the rod-GVD which is two dimensional and hence not a roadmap (The rod-GVD was termed the Voronoi complex in [13]). Second, based on the rod-GVD, we define the rod-GVG, which is one-dimensional, but not necessarily connected in a connected component of the free space and thus is not a roadmap. Finally, in the next section, we define an additional structures, which when combined with the rod-GVG, form a roadmap termed the rod-HGVG.

A. Rod-GVD

The basic building block of the rod-GVD is the set of *rod configurations* equidistant to two sets C_i and C_j, which we term the configuration two-equidistant surface

$$\mathcal{CS}_{ij} = \{q \in SE(2) : D_i(q) = D_j(q) > 0\}. \tag{2}$$

Of particular interest is the subset of $\mathcal{CS}_{ij}$, termed the configuration two-equidistant surjective surface,

$$\mathcal{CSS}_{ij} = \{q \in \mathcal{CS}_{ij} : \nabla D_i(q) \neq \nabla D_j(q)\} \tag{3}$$

which is the set of configurations, q, that are equidistant to two objects such that $\nabla D_i(q) \neq \nabla D_j(q)$. For configurations q where $\nabla D_i(q) \neq \nabla D_j(q)$, the function $\nabla(D_i - D_j)(q)$ is guaranteed to be surjective. Loosely speaking, this definition is required to deal with nonconvex sets that are modeled as the union of convex sets. More technically, the pre-image theorem requires this inequality condition to guarantee that configuration two-equidistant surjective surfaces are indeed co-dimension one. In other words, these surfaces are two-dimensional submanifolds of $SE(2)$.

The configuration two-equidistant face

$$\begin{aligned}\mathcal{CF}_{ij} =& \{q \in \mathrm{cl}(\mathcal{CSS}_{ij}) : \\ D_i(q) =& D_j(q) \leq D_h(x) \quad \forall h \neq i, j\}\end{aligned} \tag{4}$$

is the set of configurations equidistant to obstacles C_i and C_j, such that each point in $\mathrm{cl}(\mathcal{CSS}_{ij})$ is closer to C_i and C_j than any other obstacle. See Fig. 5 for examples of rods whose configurations are in configuration two-equidistant faces.

The rod generalized Voronoi diagram (rod-GVD) is the union of all configuration two-equidistant faces, i.e.,

$$\text{rod-GVD} = \bigcup_{i=1}^{n-1} \bigcup_{j=i+1}^{n} \mathcal{CF}_{ij}. \tag{5}$$

B. Rod-GVG

Consider the intersection of two configuration two-equidistant surfaces in $SE(2)$. Assuming the intersection is *transversal* [19], two two-dimensional manifolds intersect to form a one-dimensional manifold in $SE(2)$. Our goal is to create a network of one-dimensional manifolds that will form our roadmap. The pre-image theorem (with the transversality assumption) assure us that when $\mathcal{CF}_{ik}$ and $\mathcal{CF}_{ij}$ intersect, the result is nominally a one-dimensional manifold where $D_i(q) = D_j(q) = D_k(q)$. In actuality, the one-dimensional manifold is the three-way intersection of $\mathcal{CF}_{ik}$, $\mathcal{CF}_{ij}$ and $\mathcal{CF}_{jk}$. One would think that intersecting two configuration equidistant faces is sufficient, but we require the additional intersection to enforce that all gradient vectors are indeed not equal to each other. Accordingly, one can define the configuration three-equidistant face

$$\mathcal{CF}_{ijk} = \mathcal{CF}_{ij} \bigcap \mathcal{CF}_{ik} \bigcap \mathcal{CF}_{jk} \tag{6}$$

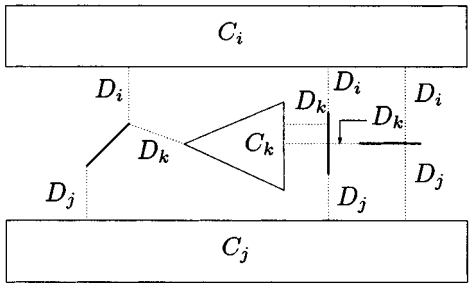

Fig. 6. The thick solid lines represent three configurations of the rod whose configurations are in the rod-GVG edge defined by obstacles C_i, C_j and C_k. The thin dotted lines represent the distance between the rods and an obstacles.

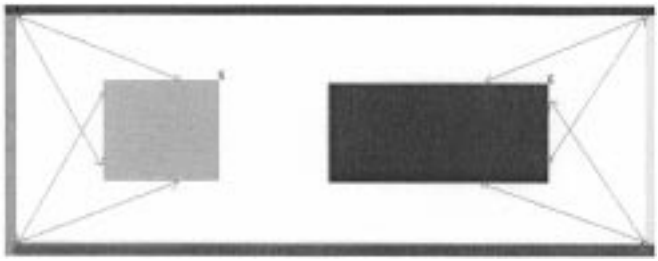

Fig. 7. Placements of rod touching obstacles correspond to rod boundary configurations. Note that at these configurations, the rod touches three obstacles, i.e., the rod is three-way equidistant at a distance of zero.

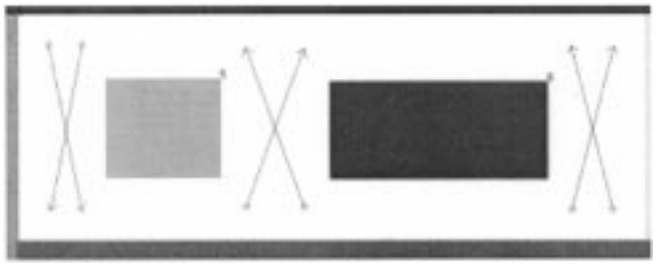

Fig. 8. Diagonal placements of rod correspond to rod meet configurations, configurations of the rod that are four-way equidistant.

to be the set of configurations where the rod is equidistant to three obstacles. For rod configurations in $SE(2)$, we term $\mathcal{CF}_{ijk}$ as a rod-GVG edge[3] (Fig. 6).

A rod-GVG edge may be C^2-homeomorphic to S^1 or a one-dimensional manifold with zero-dimensional boundary end-points. In the latter case, the end-points of the rod-GVG edges are boundary configurations and/or meet configurations. The rod-boundary configurations are configurations where the distances to the three closest objects is zero. Fig. 7 contains examples of rods placed at boundary configurations. These configurations correspond to the end-points of the "spikes" in the point-GVG. Next, the configuration four-equidistant face is defined by the intersection of rod-GVG edges, i.e., $\mathcal{CF}_{ijkl} = \mathcal{CF}_{ijk} \bigcap \mathcal{CF}_{ikl} \bigcap \mathcal{CF}_{ikl} \bigcap \mathcal{CF}_{jkl}$. For rod configurations in $SE(2)$, $\mathcal{CF}_{ijkl}$ is a rod meet configuration. Fig. 8 contains configurations of rods at rod meet configurations. The rod meet configurations and boundary configurations are

[3] O'Dúnlaing and Yap [13] define their one-dimensional three-way equidistant structure when the race-track surrounding the rod touches three or more obstacles.

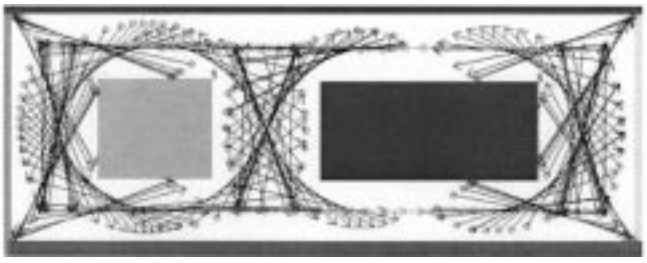

Fig. 9. Placements of a long rod along the rod-GVG, which, in this figure, is connected.

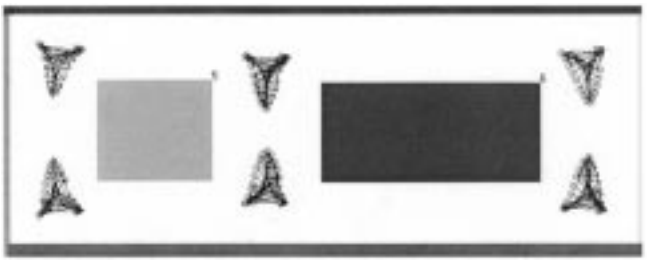

Fig. 10. Placements of a short rod along the rod-GVG, which, in this figure, is not connected.

the end points of the rod-GVG edges. With these structures in hand, we can define the rod-GVG.

Definition 3: The **rod-GVG** is a collection of edges comprising rod-GVG edges and nodes comprising rod-meet configurations and rod-boundary configurations.

Fig. 9 displays the "swept volume" of the rod as it passes through the rod-GVG for the rod in the environment demonstrated in Figs. 7 and 8. Here, the resulting rod-GVG is connected. That that all of the rod-GVG edges have end points: meet configurations and boundary configurations. Fig. 10 contains the swept volume of a smaller rod robot in a the same environment. There are no rod-meet nor rod-boundary configurations in this example and the rod-GVG edges are diffeomorphic to S^1.

We use standard numerical construction techniques to construct the rod-GVG by simply tracing the roots of the expression

$$G_{\text{rod}}(q) = \begin{bmatrix} D_i(q) - D_j(q) \\ D_i(q) - D_k(q) \end{bmatrix}. \tag{7}$$

When $G_{\text{rod}}(q) = 0$, we have $D_i(q) = D_j(q)$ and $D_i(q) = D_k(q)$ and hence by transitivity, $D_j(q) = D_k(q)$. This gives us a rod-GVG edge configuration q where $D_i(q) = D_j(q) = D_k(q)$. A key feature here is that $G_{\text{rod}}(q)$ is defined in terms of the rod-distance function which can determined from range sensor readings, as described in Section III. In other words, using work space distance measurements, we can construct the rod-GVG edge in configuration space. The explicit derivation of the curve tracing technique can be found in the Appendix.

V. Accessibility: Retraction of a Junction Region

Recall that a roadmap is a one-dimensional network of curves that have the properties of accessibility, connectivity and departability in each connected component of the free space. *Accessibility* is the property that the rod can move from any configuration in the workspace to a configuration on a rod-GVG

edge. He, we demonstrate that the rod-GVG (by itself) has the accessibility property, but we use this result as a building block for the connectivity proof in a later section. The accessibility algorithm described below prescribes a path to a rod-GVG edge such that the rod moves with a fixed orientation. In a sense, this reduces the problem to accessibility of a point in a planar configuration space because the configuration space of a rod with a fixed orientation is $\mathbb{R}^2$.

Rod accessibility is achieved in two steps. Let C_i be the closest obstacle to a rod R. While maintaining a fixed orientation, the rod moves away from C_i until it is double equidistant with object C_j. In other words, it follows a path

$$\dot{c}_1(t) = \tilde{\nabla} D_i(c_1(t)).$$

Once the rod robot achieves double equidistance, it then moves away from the two closest objects, while maintaining double equidistance, until the rod attains triple equidistance to objects C_i, C_j and C_k. So, the robot follows a path

$$\dot{c}_2(t) = \pi_{T_{c_2(t)}\mathcal{CF}_{ij}} \tilde{\nabla} D_i(c_2(t))$$

where π is the projection operator and $\pi_{T_{c_2(t)}}$ projects onto the tangent space $T_{c_2(t)}$. Alternatively, this path can be defined as $\dot{c}_2(t) = \pi_{T_{c_2(t)}\mathcal{CF}_{ij}} \tilde{\nabla} D_j(c_2(t))$ because $\pi_{T_q\mathcal{CF}_{ij}} \tilde{\nabla} D_i(q) = \pi_{T_q\mathcal{CF}_{ij}} \tilde{\nabla} D_j(q)$.

Proposition 1: (Rod Accessibility) In a bounded environment, the rod-GVG has the accessibility property for almost all configurations in the rod's free space.

Proof: Without loss of generality, assume the rod lies in a configuration q_1 that is closest to obstacle C_i. Given that the rod is located in a bounded space, continuity of the distance function ensures that when the rod follows a path $\dot{c}_1(t) = \tilde{\nabla} D_i(c_1(t))$ it will arrive at a configuration q_2 where object C_j is equidistant to C_i, i.e., $D_i(q_2) = D_j(q_2)$.

Let $D(q) = \min_h D_h(q)$. Using the results in nonsmooth analysis [10], [20], it can be shown that $\pi_{T_q\mathcal{CF}_{ij}} \nabla D_i(q) = \pi_{T_q\mathcal{CF}_{ij}} \nabla D_j(q)$, both of which are equal to the generalized gradient of D projected onto $T_q\mathcal{CF}_{ij}$. Therefore, as long as $\pi_{T_q\mathcal{CF}_{ij}} \nabla D_i(q)$ (or $\pi_{T_q\mathcal{CF}_{ij}} \nabla D_j(q)$) does not vanish, continuity of D ensures that the path $\dot{c}_2(t) = \pi_{T_{c_2(t)}\mathcal{CF}_{ij}} \tilde{\nabla} D_i(c_2(t))$ will reach a configuration q_3 where $D_i(q_3) = D_j(q_3) = D_k(q_3)$, i.e., a configuration on the rod-GVG.

When obstacles lie in general position, there will be an isolated configuration q^* that is a local minimum of D on $\mathcal{CF}_{ij}$, i.e., $\pi_{T_{q^*}\mathcal{CF}_{ij}} \nabla D_i(q^*) = 0$ [5] for a nongeneric configuration q^*. In this scenario, the rod configuration needs to be slightly perturbed in order to escape the local minimum using gradient ascent. If the obstacles are not in general position, then there is a connected set of configurations in $\mathcal{CF}_{ij}$ that form a degenerate local minimum. In this scenario, the rod robot need only to move in a fixed direction until it escapes the set of minima.

Thus far, we have defined the rod-GVG and demonstrated that all configurations in the free space can access a configuration on the rod-GVG. However, there is more structure and detail to be exploited in the accessibility procedure that we can use to demonstrate connectivity later on. We will show below that all configurations that access the same connected component of a rod-GVG edge form a connected set. With this in mind, we define the a *junction region* $\mathcal{J}_{ijk}$, as the set of configurations that access the rod-GVG edge $\mathcal{CF}_{ijk}$. Note that neither $\mathcal{J}_{ijk}$ nor $\mathcal{CF}_{ijk}$ is guaranteed to be connected. The goal is to show that each connected $\mathcal{CF}_{ijk}$ has an associated connected $\mathcal{J}_{ijk}$. So, we will then show that $\mathcal{CF}_{ijk}$ is a retract of $\mathcal{J}_{ijk}$. This result will be useful in demonstrating connectivity of the rod roadmap.

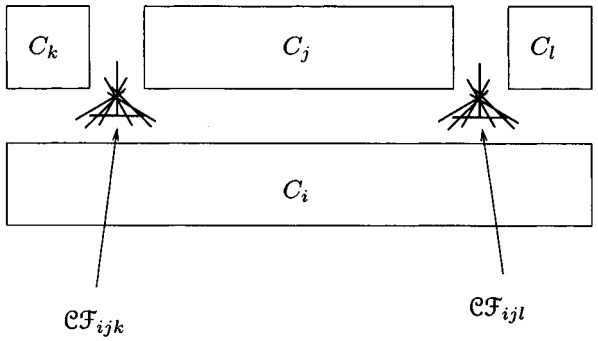

Fig. 11. The two clusters of solid lines represent rods whose configurations are triply equidistant to three obstacles. The left cluster represents rods whose configurations are elements of the rod-GVG edge $\mathcal{CF}_{ijk}$ and the right cluster are elements of $\mathcal{CF}_{ikl}$. In this example, both rod-GVG edges are diffeomorphic to S^1 (i.e., they are cyclic) and neither rod-GVG edge is connected to any other rod-GVG edge.

Lemma 1: The set of all configurations that access the same connected component of a rod-GVG edge form a connected set.

Proof: Let q_1 and q_2 be two arbitrary configurations that access the same connected component of a rod-GVG edge, $\mathcal{CF}_{ijk}$ at configurations q_1^* and q_2^*. By definition, both configurations lie in the same junction region $\mathcal{J}_{ijk}$. There is a path from q_1 to q_1^* and then to q_2^* and finally to q_2 that is fully contained in $\mathcal{J}_{ijk}$. Since q_1 and q_2, were arbitrary, all configurations which access the same connected component of a rod-GVG edge form a connected set.

We are now going to develop a retraction H for each connected component of a junction region using the accessibility criterion:

Corollary 1: There exists a continuous map $H : \mathcal{J}_{ijk} \times [0,1] \rightarrow \mathcal{J}_{ijk}$ where $H(q,t)$ describes the rod accessibility path starting at a configuration $q = H(q,0) \in \mathcal{J}_{ijk}$ and arriving at $q' = H(q,1) \in \mathcal{CF}_{ijk}$.

See the Appendix for the proof of this corollary. The union of the closure of the junction regions fills the configuration space, but their is some ambiguity about the common boundary of adjacent junction regions. For the ease of notation, assume that the rod can access either rod-GVG edge associated with the shared boundary of adjacent junction regions. This assumption is reasonable because the boundaries of junction regions form a set of measure zero and any slight perturbation from this set automatically puts the rod in a specific junction region.

VI. The Rod-HGVG

It was shown in [13] that the configuration rod-GVD is connected. However, the rod-GVG is not necessarily connected as can be seen in Fig. 11. In order to connect the rod-GVG, we define additional structures, termed R-edges, that link disconnected rod-GVG edges by exploiting the property that the point

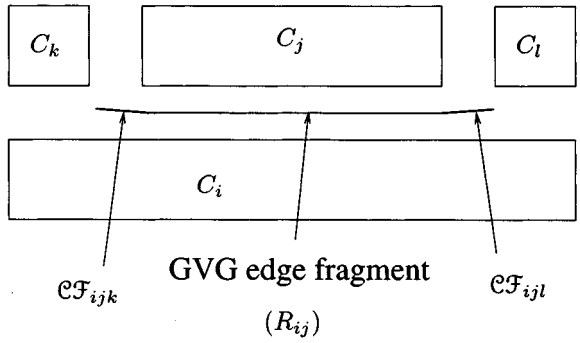

Fig. 12. The dark line segment on the left represents a rod configuration in $\mathcal{CF}_{ijk}$ and the dark segment on the right represents a rod configuration in $\mathcal{CF}_{ijl}$. These rods are connected by the point GVG edge $\mathcal{F}_{ij}$. The point GVG edge gives rise to a linking structure termed the R-edge which connects $\mathcal{CF}_{ijk}$ and $\mathcal{CF}_{ijl}$.

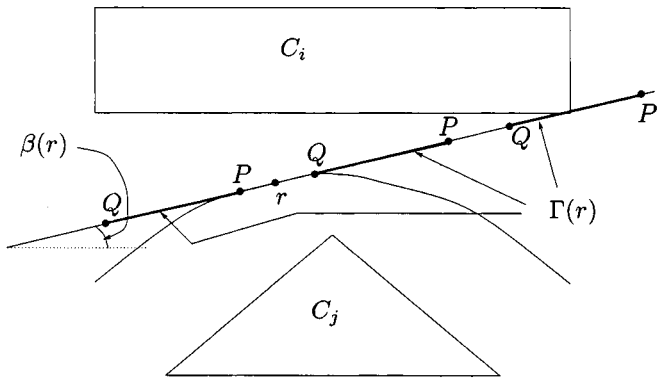

Fig. 13. The solid lines delineate three configurations of a rod that lie in $\Gamma(r)$. $\beta(r)$ is the angle which describes the tangent space to the point GVG edge at the point r.

GVG is connected in the plane. See Fig. 12. The R-edges are the set of rod configurations that correspond to placements of the rod $R(q)$ that are tangent to the point-GVG edge. The point of tangency with the rod, as described below, is "normally" one of the rod end points, P or Q, except when the rod passes through the isolated point $r_{\min}$ on the point-GVG edge $\mathcal{F}_{ij}$ that is a local minimum of d_i (or d_j) restricted to $\mathcal{F}_{ij}$. In this case, the rod "slides" through $r_{\min}$ maintaining tangency with $\mathcal{F}_{ij}$. See Fig. 14.

In formally defining the R-edges, we pay careful attention to embedding the tangent space of the point-GVG edge into the configuration space of the rod. Note that this requires us to introduce some notation which we use to prove that the R-edges are indeed one-dimensional and yield the result that the rod is tangent at P or Q except at the local minimum. Next, we introduce two lemmas that echo the results of [5] that connect disconnected point-GVG networks. Finally, in this section, we describe an algorithm for constructing the rod-HGVG. In the next section, we discuss connectivity.

A. Definition and Dimension Count of R-Edges

Recall that the tangent space of a planar point-GVG edge is the line orthogonal to the line segment which connects the nearest points of the two nearest obstacles which locally define the point GVG edge [6]. Let $C_i(r)$ be the closest obstacle to a point r in the plane. In this vein, let c_i be the vector which connects r and the closest point to r on the closest obstacle $C_i(r)$.

We define a mapping $\beta(r)$ that describes the tangent space of a point-GVG edge at a point r, so that we can embed this tangent space into the workspace of the robot. Let $\beta : \mathcal{SS}_{ij} \rightarrow S^1$ be defined as

$$\beta(r) = \text{arctangent}(c_i(r) - c_j(r)) + \frac{\pi}{2} \tag{8}$$

where $\pi/2$ is measured in radians. It can be shown that $c_i(r)$ is a continuous function for convex sets [12] and thus β is a continuous function.

Let the mapping $\Gamma : \mathcal{SS}_{ij} \rightarrow SE(2)$ be defined as

$$\Gamma(r) = \left\{ \begin{matrix} r^x + l\cos(\beta(r)) \\ r^y + l\sin(\beta(r)) \\ \beta(r) \end{matrix} : l \in \mathbb{R}^1 \right\}. \tag{9}$$

It can easily be seen that Γ is a continuous mapping. $\Gamma(r)$ can be viewed as all the rods that lie in the tangent space of a two-equidistant surjective surface (and thus a two-equidistant face) at a point r. See Fig. 13 for an example of $\Gamma(r)$.

Let the R-two-equidistant surjective surface defined by C_i and C_j be

$$R\mathcal{SS}_{ij} = \{\Gamma(r) : r \in \mathcal{SS}_{ij}\}. \tag{10}$$

Since $R\mathcal{SS}_{ij} \simeq \mathcal{SS}_{ij} \times \mathbb{R}^1$, the dimension of $R\mathcal{SS}_{ij}$ is two (recall that in $\mathbb{R}^2$, the dimension of $\mathcal{SS}_{ij}$ is one [5]). $R\mathcal{SS}_{ij}$ may be viewed as (but is not) a tangent bundle of $\mathcal{SS}_{ij}$.

Let the R-two-equidistant face be the set of configurations equidistant to two obstacles such that **(I)** there exists a point, $r \in R$, that is closer to obstacles C_i and C_j than any other point on the rod and **(II)** no other obstacle is closer to the rod than the two equidistant obstacles. In other words,

$$\begin{aligned} R\mathcal{F}_{ij} = \{&q \in \text{cl}(R\mathcal{SS}_{ij}) : \text{ such that } \exists r \in R(q) \\ &(\mathbf{I})\ d_i(r) \le d_i(r_1)\ \forall r_1 \in R(q) \\ &\text{and } \ d_j(r) \le d_j(r_1) \ \text{ and} \\ &(\mathbf{II})\ d_i(r) \le D_h(q)\ \forall h \ne i,j\}. \end{aligned} \tag{11}$$

In $SE(2)$, an R-two-equidistant face is termed an R-edge, (denoted $\mathcal{R}_{ij}$) because it is one-dimensional, as shown by the following proposition.

The inequality $\mathbf{I}\ \boldsymbol{d_i(r) \le d_i(r_1)\ \forall r_1 \in R(q)}$ determines how the rod is tangent to the point GVG edge. Let $r_{\min}$ be the point in $\mathcal{F}_{ij}$ where the distance to C_i and C_j is the smallest (i.e., for all $r \in \mathcal{F}_{ij}\backslash\{r_{\min}\}$, $d_i(r) > d_i(r_{\min})$). For all points $r \in \mathcal{F}_{ij}\backslash\{r_{\min}\}$, the rod is tangent to the point GVG edge at P or Q. Otherwise at $r_{\min}$, the rod is free to slide along the tangent space of the point GVG edge. See Figs. 14 and 15.

Proposition 2: The R-edges are one dimensional in $SE(2)$.

Proof: Assume without loss of generality that obstacles C_i and C_j have one unique pair of closest points, c_i and c_j. Let the distance between these two points be $2D_{\min}$. Therefore, for all points $c_1 \in C_i\backslash\{c_i\}$ and for all points $c_2 \in C_j$, $\|c_1 - c_2\| > 2D_{\min}$. This assumption implies that there exists a unique point, $r_{\min} \in \mathcal{SS}_{ij}$, where $d_i(r_{\min}) = d_j(r_{\min}) = D_{\min}$ and for all other points $r \in \mathcal{SS}_{ij}\backslash\{r_{min}\}$, $d_i(r) = d_j(r) > d_i(r_{\min}) = d_j(r_{\min})$.

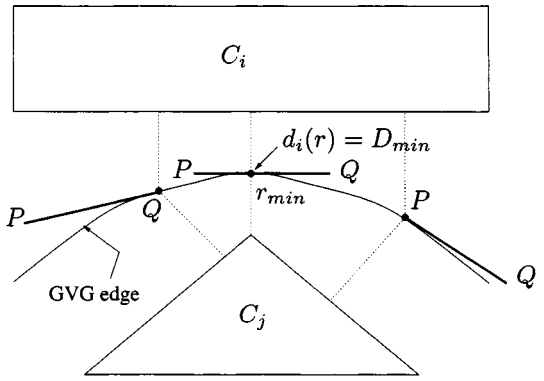

Fig. 14. The rod is moving from left to right while remaining tangent to the point GVG edge defined by obstacles C_i and C_j. The thick solid lines represent different configurations of the rod in an R-edge. The dotted lines represent the shortest distance between the rod and the nearby obstacles. Note, for all configurations where the rod is *not* tangent to r the closest point on the rod to C_i and C_j is either P or Q.

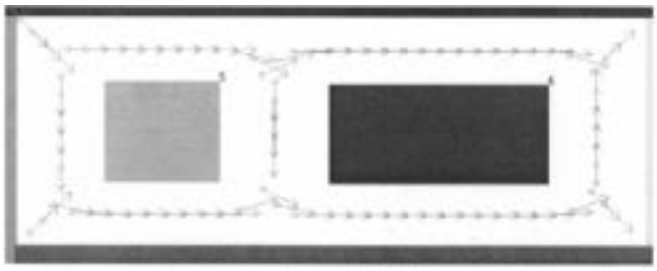

Fig. 15. Placements of rod along the R-edges for the environment in Fig. 10.

The proof follows in two steps. First, we show that for all configurations $q \in R\mathcal{F}_{ij}$ where $d_i(r) > D_{\min}$, there exists a unique configuration of the rod that is tangent to the point-GVG and that satisfies the inequalities in (11) (in fact, $d_i(r) = D_i(q)$). Second, we show that the set of configurations where $D_i(q) = D_{\min}$ forms a one-dimensional curve in $SE(2)$.

Consider the case where $d_i(r) > D_{\min}$. Assume the point of contact r is neither $P(q)$ nor $Q(q)$. By (11), $D_i(q) = d_i(r)$ which is greater than $D_{\min}$, by hypothesis. Let the projection of the distance gradient at r onto the rod be $\pi_{R(q)}\nabla d_i(r)$. We know $\pi_{R(q)}\nabla d_i(r)$ does not vanish because $D_i(q) > D_{\min}$, i.e., $d_i(r)$ restricted to the rod never obtains a local minimum in its interior because d_i is a convex function defined on a convex set (the rod) and all values of d_i are greater than $D_{\min}$.

Hence, $-\pi_{R(q)}\nabla d_i(r) \neq 0$ and there exists a $y \in \text{nbhd}(r) \bigcap R(q)$ such that $d_i(y) < d_i(r)$. This violates the inequality, $d_i(r) \leq d_i(r_1)\ \forall r_1 \in R(q)$ (from (11)). Thus, the only points for which the rod may intersect $\mathcal{SS}_{ij}$ and maintain the inequality, $d_i(r) \leq d_i(r_1)\ \forall r_1 \in R(q)$, is either $P(q)$ or $Q(q)$. Therefore, all configurations $q \in \mathcal{CSS}_{ij}$ that satisfy the inequality, $d_i(r) \leq d_i(r_1)\ \forall r_1 \in R(q)$, can be identified with $\mathcal{SS}_{ij} \times \{P(q)\}$ or $\mathcal{SS}_{ij} \times \{Q(q)\}$, both of which are one-dimensional.

Now, consider the case where $d_i(r_{\min}) = d_j(r_{\min}) = D_{\min}$. $\pi_{R(q)}\nabla d_i(r_{\min})$ vanishes for the set of configurations where $d_i(r_{\min}) = d_j(r_{\min}) = D_{\min}$. Thus, for all configurations of the the rod where $r_{\min} \bigcap R(q) = r_{\min}$, there always exists a neighborhood, $\text{nbhd}(r_{\min}) \bigcap R(q)$, where $d_i(y) \geq d_i(r_{\min})$ for all $y \in \text{nbhd}(r_{\min}) \bigcap R(q)$. Therefore, all such configurations can be identified with $\{r_{\min}\} \times [0, L]$ which is also one-dimensional.

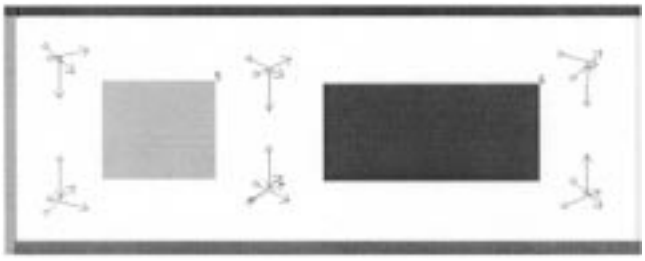

Fig. 16. Placements of rod along the rod-GVG where R-edges intersect them.

The inequality $d_i(r) \leq D_h(q)\ \forall h \neq i, j$ forces the rod to be closest to obstacles C_i and C_j, but does not affect the dimensionality of the edges.

The incremental construction technique of the R-edges is the same as the incremental construction procedure for point GVG edges (described in [6]), which is amenable to sensor-based implementation. Hence, the R-edges can be constructed in an incremental fashion using only line of sight information.

B. Definition and Algorithm for the Rod-Hierarchical Generalized Voronoi Graph

Definition 4: (Rod-HGVG) The rod hierarchical generalized Voronoi graph (rod-HGVG) is the collection of rod-GVG edges and R-edges.

The following two lemmas indicate that a linking strategy using the R-edges echos the linking strategy defined by the second order GVG for the point-GVG in higher dimensions [5].

Lemma 2: The R-edges are subsets of configuration two-equidistant faces.

Proof: Recall that for all configurations $q \in \mathcal{R}_{ij}$, there exists an $r \in R(q)$ such that $d_i(r) \leq d_i(r_1)$ and $d_j(r) \leq d_j(r_1)$ for all points $r_1 \in R(q)$. Since $D_i(q) = \min_{r \in R(q), c \in C_i} \|r - c\|$, $d_i(r) = D_i(q)$ and $d_j(r) = D_j(q)$. Therefore for all configurations $q \in \mathcal{R}_{ij}$, $D_i(q) = D_j(q)$ and thus for all $q \in \mathcal{R}_{ij}$, $q \in \mathcal{CF}_{ij}$.

Lemma 3: For all configurations $q \in \mathcal{R}_{ij}$, the rod does not intersect any obstacle (with the exception of points P or Q lying on the intersection of two obstacles).

Proof: By definition, for all $q \in \mathcal{R}_{ij}$, there exists $r \in R(q)$ such that $d_i(r_1) \geq d_i(r)$ for all $r_1 \in R(q)$. Since $d_i(r) \geq 0$, for all $r_1 \in R(q)$, $d_i(r_1) > 0$ because we assume the rod does not fully intersect an obstacles boundary. Thus, with perhaps the exception of the point P or Q, the rod does not intersect an obstacle.

By definition of the R-edges, it can be easily seen that the terminating conditions of an R-edge are either on the boundary of the environment or when the rod is equidistant to three obstacles, i.e., a point on a rod-GVG edge. See Fig. 16.

The algorithm for constructing the rod-HGVG is rather straightforward; essentially it is a graph search of configuration space. The robot accesses the rod-GVG from any configuration using the accessibility criterion. It identifies the configuration where it accessed the rod-GVG as a node and then incrementally constructs the rod-GVG edge until it re-encounters the access

node or a rod meet configuration. All nodes are put on a queue. While generating the rod-GVG, the robot also marks as nodes the configurations where R-edges intersect the rod-GVG edge. These nodes are also put on a queue. The robot then generates the unexplored edge, either an R-edge or another rod-GVG edge, associated with the first node on the queue which is taken off the queue when all edges emanating from the node are explored. If new nodes, other than boundary configurations, are encountered these nodes are placed on the queue as well. When a boundary configuration is encountered, the robot simply terminates tracing and goes to the next node on the queue. Exploration is complete when there are no nodes left on the queue, i.e., all nodes have no unexplored edges emanating from them.

VII. Connectivity of the Rod-HGVG

Proposition 3: Let q_1 and q_2 be two configurations of the rod. There exists a path between q_1 and q_2 if and only if there exists a path on the rod-HGVG between $H(q_1,1)$ and $H(q_2,1)$ where H is the function which describes the accessibility path of the rod from an initial configuration to a configuration on the rod-GVG.

Proof: First we show the converse of this statement. By Proposition 1 and Corollary 1, there exists a path between q_1 and $H(q_1,1)$ and there exists a path between q_2 and $H(q_2,1)$. If there exists a path from $H(q_1,1)$ to $H(q_2,1)$ on the rod-HGVG, then there exists a path between q_1 and q_2.

Next, we show that if there exists a path between q_1 and q_2, then there exists a path between $H(q_1,1)$ and $H(q_2,1)$ on the rod-HGVG. If $q_1 \in \mathcal{J}_{ijk}$ and $q_2 \in \mathcal{J}_{pqr}$ and there exists a path between them, then there exists a series of adjacent junction regions, $\mathcal{J}_{ijk}, \mathcal{J}_{ijl}, \ldots, \mathcal{J}_{pqr}$ through which this path passes.

The problem of connectivity is now reduced to demonstrating that: (i) if two R-edges intersect a configuration three-equidistant face, $\mathcal{CF}_{ijk}$, then there exists a path between the two edges if and only if there exists a path between the two edges on $\mathcal{CF}_{ijk}$ and (ii) there exists a path between two rod-GVG edges in adjacent junction regions if and only if there exists an R-edge that links the two rod-GVG edges.

Lemma 4: Let $\hat{q}_1, \hat{q}_2$ be two configurations in a junction region $\mathcal{J}_{ijk}$. $\hat{q}_1$ and $\hat{q}_2$ are path connected within a junction, $\mathcal{J}_{ijk}$, if and only if $H(\hat{q}_1,1)$ and $H(\hat{q}_2,1)$ are path connected in $\mathcal{CF}_{ijk}$.

Proof: By definition, $\mathcal{CF}_{ijk} \subset \mathcal{J}_{ijk}$. By Proposition 1 and Corollary 1, there exists a path between $\hat{q}_1$ and $H(\hat{q}_1,1)$ and there exists a path between $\hat{q}_2$ and $H(\hat{q}_2,1)$. Therefore, if there exists a path between $H(\hat{q}_1,1)$ and $H(\hat{q}_2,1)$ in $\mathcal{CF}_{ijk}$, then there exists a path between $\hat{q}_1$ and $\hat{q}_2$ in $\mathcal{J}_{ijk}$.

Recall from Corollary 1 that there exists a continuous function, $H(q,t)$ which describes the accessibility for the rod.

Let $s(t)$ be a continuous function which describes a path from $\hat{q}_1$ to $\hat{q}_2$ such that $s(0) = \hat{q}_1$ and $s(1) = \hat{q}_2$. For all $t \in [0,1]$, $H(s(t),1) \in \mathcal{CF}_{ijk}$. The image of the path between $\hat{q}_1$ and $\hat{q}_2$ under $H(s(t),1)$ is a connected path on $\mathcal{CF}_{ijk}$ because the image of a connected set under a continuous mapping is a connected set.

Now, it needs to be shown that the R-edges connect the rod-GVG edges in adjacent junction regions. The following proposition guarantees that there exists a path between two adjacent rod-GVG edges if and only if there exists a connected R-edge linking them.

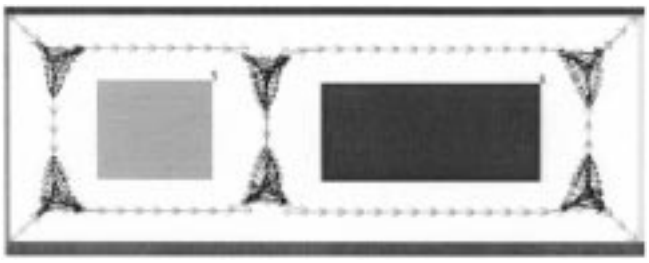

Fig. 17. Placements of rod along the rod-HGVG.

Lemma 5: Let $\bar{q}_1 \in \mathcal{CF}_{ijk}$ and $\bar{q}_2 \in \mathcal{CF}_{ijl}$ such that $\bar{q}_1$ and $\bar{q}_2$ are also on an R-edge, $\mathcal{R}_{ij}$, $\mathcal{CF}_{ijk}$ and $\mathcal{CF}_{ijl}$ are in adjacent junctions regions. $\bar{q}_1$ and $\bar{q}_2$ are path connected if and only if the R-edge between them is connected.

Proof: If $\bar{q}_1$ and $\bar{q}_2$ lie on a connected R-edge then there exists a path between $\bar{q}_1$ and $\bar{q}_2$.

If there exists a path between $\bar{q}_1$ and $\bar{q}_2$, then there exists a point based GVG edge, $\mathcal{F}_{ij}$, which connects $[\bar{q}_1^x, \bar{q}_1^y]^T$ and $[\bar{q}_2^x, \bar{q}_2^y]^T$ in the plane. The R-edge which connects $\bar{q}_1$ and $\bar{q}_2$ is the image of a connected subset of $\mathcal{F}_{ij}$, which connects $[\bar{q}_1^x, \bar{q}_1^y]^T$ and $[\bar{q}_2^x, \bar{q}_2^y]^T$, under Γ. The R-edge is a connected set because the image of a connected set under a continous function is a connected set. Lemma 3 guarantees that all configurations of the rod on the R-edge do not intersect any other obstacle.

By Lemmas 4 and 5, if there exists a path between q_1 and q_2, then there exists a path between $H(q_1,1)$ and $H(q_2,1)$ and thus the rod-HGVG is connected.

From Section V, we demonstrated that the rod-GVG and hence the rod-HGVG (because the rod-GVG is a subset of the rod-HGVG) has the accessibility property and Proposition 3 ensures the rod-HGVG has the connectivity property, making the rod-HGVG a roadmap in the classical sense. From [6], it can be shown that at least one point from a configuration on the rod-HGVG will be within line of sight of at least one point from any configuration in the free space and hence the rod-HGVG has the departability property. Therefore, the rod-HGVG is a roadmap. See Fig. 17 for an example of a rod-HGVG.

VIII. Discussion

A. Comparison of Point-HGVG and Rod-HGVG

The rod-HGVG has inherited properties from both the planar and three-dimensional HGVG for a point. By definition, just like the point-GVG in $\mathbb{R}^3$, the rod-GVG is triple equidistant to three objects because $\mathbb{R}^3$ and $SE(2)$ are both three-dimensional. Also, the point-GVG in $\mathbb{R}^3$ and the rod-GVG are not guaranteed to be connected and thus additional structures are defined to connect them. In the case of the point GVG, second order GVG edges connect the GVG whereas the R-edges link rod-GVG edges.

However, the structure of the rod-HGVG is simpler than that of the point-HGVG because the rod-GVG does not contain occluding edges. Occluding edges are structures in the point-HGVG that represent positions where obstacles appear

and disappear; i.e., points where obstacles become occluded or unoccluded. Typically, occluding edges appear "on top of" or "below" obstacles in three-dimensions. The rod-HGVG does not have occluding edges because the rod completely lies in the plane and hence never has to "go over" anything in order to ensure completeness.

B. No Strong Deformation Retract

Recall that the planar point-GVD is a retract of the plane [12]. This is desirable because a retract (continuously) captures the topology of the robot's environment and thus for each connected component of the free space, there is a connected retract. Unfortunately, three dimensional spaces populated with obstacles in general do not have one-dimensional retracts because there does not exist in general a function that maps the three-dimensional manifold to a one-dimensional manifold that is continuous *and* the identity on the one-dimensional manifold. Instead, we divided the configuration space into a cellular decomposition where there exists a retraction in each three-dimensional cells. The junction regions are the cells and the rod-GVG edges are the retracts of the junction regions. We then used R-edges to link adjacent cells, thereby forming a roadmap (which is not a retract) of $SE(2)$.

C. Rod HGVG Depends Upon Choice of Body Frame

It is interesting to note that full gradient definition $\nabla D_i(q)$ reflects the lack of bi-invariance of all metrics in $SE(2)$ and $SE(3)$ [21]. A *left-invariant* metric in $SE(3)$ is one for which given any two points $p_1, p_2 \in SE(3)$, the distance between these points, $d(p_1, p_2)$, is the same as $d(Tp_1, Tp_2)$ for all $T \in SE(3)$. This means, changing the location of the world coordinate frame does not change the distance between two points in $SE(3)$. A *right-invariant* metric in $SE(3)$ is one for which given any two two points $p_1, p_2 \in SE(3)$, the distance between these points, $d(p_1, p_2)$, is the same as $d(p_1T, p_2T)$ for all $T \in SE(3)$. This means that changing the location of the body fixed coordinate frame does not affect the distance between two points in $SE(3)$. It was shown in [21] that no metric in $SE(3)$ can be both left-invariant and right-variant, i.e., no metric in $SE(3)$ can be bi-invariant. Note that the gradient in (19) depends upon the choice of a body-fixed coordinate frame; this reflects the lack of bi-invariance in $SE(2)$ and $SE(3)$.

The definition of the rod-HGVG uses the gradient in (19). This means that the rod-HGVG depends upon the choice of the body-fixed frame. This is consistent with the configuration space formulation [22] which also depends upon the choice of the body-fixed frame. So, just as the configuration space depends upon the choice of a body-fixed frame, so should a roadmap of that space.

IX. Conclusion

This paper introduces a retract-like structure called the *rod hierarchical generalized Voronoi graph* (rod-HGVG). Using the rod-HGVG, a planar rod-shaped robot can plan a path between any two configurations, q_{start} and q_{goal}. The rod-HGVG can be viewed as a one-dimensional graph embedded in a three-dimensional configuration space $SE(2)$. Since a bulk of the motion planning occurs on the rod-HGVG, a search algorithm between two configurations is reduced from a three-dimensional search to a one-dimensional one.

Since the rod-HGVG is defined in terms of work space distance measurements, it can be constructed using sensor data. This paper provides a derivation of a distance function and its gradient in the configuration space $SE(2)$. Derivation of the gradient required some care because $SE(2)$ is not a Euclidean space. The gradient is not only a function of configuration but it is also a function of the body-fixed coordinate frame of the rod, which reflects the lack of bi-invariance of any metric in $SE(2)$.

Using work space distance function and the lifted gradient into configuration space, the robot can systematically generate the rod-HGVG, thereby exploring the robot's configuration space. It is worth pointing out that the robot never explicitly constructs the configuration space. Instead, the rod-robot constructs a roadmap representation of it. This is important for sensor-based planning because before it can construct the configuration space the robot needs to know its entire workspace which is not known a priori in exploration tasks. Furthermore, this approach has the added benefit of saving computational time in constructing the configuration space, which is useful even when full knowledge of the robot's environment is available.

One of this method's limitations is that it assumes there are range sensors distributed throughout the body of the rod. Discrete sensor placements should adequately approximate such a sensor distribution, but this approximation is currently being investigated. Ultimately, we will extend this paradigm to a rod flying around in a three-dimensional space which introduces an order of magnitude difficulty in determining sensor placement. Finally, there are environments where range sensor information cannot be readily provided, so a robot must rely on visual sensor data. Visual exploration using roadmaps is a current topic of research.

Another area of future research considers the nonholonomic constraints for the rod robot. Currently, we assume the rod can instantaneously translate and rotate in any direction. For a wheeled robot in cluttered workspaces, this assumption may not be reasonable. However, it is worth pointing out that the rod robot "appears" to move as if it has steerable wheels. Consider a rod moving from the far left to the right and then up between the two obstacles in Fig. 17. The rod first slides along the R-edge on the bottom of the figure, then approximates a parallel park-type maneuver to rotate in place and finally it follows the vertical R-edge to move up. Future work will demonstrate how the rod-HGVG may approximate nonholonomic constraints.

This work is the next step toward the ultimate goal of sensor-based planning for an articulated multi-body chain robot. The roadmap result here will first be extended to a rod floating in three dimensions. The next step will be to extend the rod result to that of a convex body. Once a roadmap and exploration procedure for a single convex body is accomplished, we will attempt the two-body problem and then the n-body problem (Fig. 18).

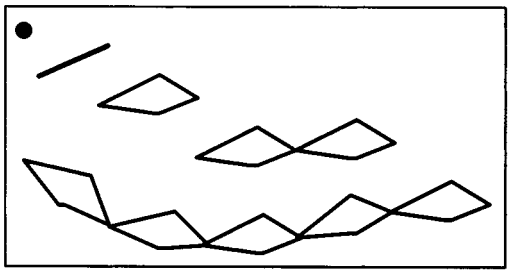

Fig. 18. Outline of future research.

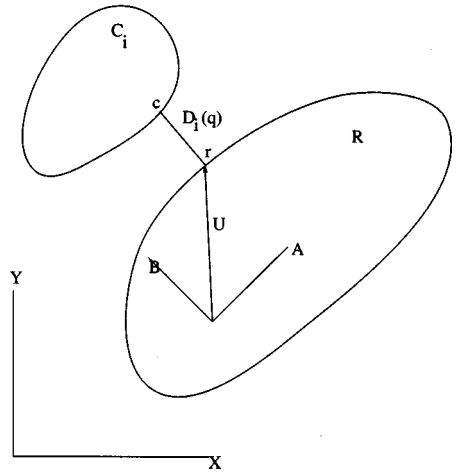

Fig. 19. Description of the variables.

APPENDIX I

A. Rod Distance Gradient

In actuality, the rod-distance function definition also applies to measuring distance between two convex sets. Therefore, this section is devoted to the gradient of the distance between two convex sets. The distance between the robot and a convex obstacle is simply the distance between the pair of closest points on the robot and obstacle. That is,

$$D_i(q) = \min_{r \in R(q), c \in C_i} \|c - r\|$$

measures the distance between a convex robot and a convex obstacle, where $q \in SE(2)$ and $R(q)$ are the set of points in $\mathbb{R}^2$ that the robot occupies. Note that this definition is identical to (1).

Assume a world coordinate frame whose axes are X and Y and a body fixed coordinate frame on R whose axes are A and B. Let $(x, y)^T$ be the origin of the body fixed coordinates in the world coordinate frame and let θ denote the orientation of the body fixed coordinate frame with respect to the world coordinate frame. Let c be the closest point on the obstacle C_i to the robot R and let r be the closest point on the robot R to the obstacle C_i. Finally, let $(a, b)^T$ be r in the body fixed coordinate frame. See Fig. 19. Therefore, the world coordinates of r is

$$\begin{aligned} r &= \begin{bmatrix} x \\ y \end{bmatrix} + \begin{bmatrix} \cos\theta & -\sin\theta \\ \sin\theta & \cos\theta \end{bmatrix} \begin{bmatrix} a \\ b \end{bmatrix} \\ &= \begin{bmatrix} x + a\cos\theta - b\sin\theta \\ y + a\sin\theta + b\cos\theta \end{bmatrix}. \end{aligned} \tag{12}$$

The distance $D_i(q)$ is $\left((c^x - r^x)^2 + (c^y - r^y)^2\right)^{1/2}$. First, consider the partial derivative with respect to x.

$$\begin{aligned} \frac{\partial D_i(q)}{\partial x} = \frac{1}{D_i(q)} \Bigg(& (c^x - r^x)\left(\frac{\partial c^x}{\partial x} - \frac{\partial r^x}{\partial x}\right) \\ & + (c^y - r^y)\left(\frac{\partial c^y}{\partial x} - \frac{\partial r^y}{\partial x}\right)\Bigg) \end{aligned} \tag{13}$$

From (12),

$$\begin{aligned} \frac{\partial r^x}{\partial x} &= 1 + \frac{\partial a}{\partial x}\cos\theta - \frac{\partial b}{\partial x}\sin\theta \\ \frac{\partial r^y}{\partial x} &= \frac{\partial a}{\partial x}\sin\theta + \frac{\partial b}{\partial x}\cos\theta. \end{aligned} \tag{14}$$

Substitute the above into $\partial D_i(q)/\partial x$ in (13).

$$\begin{aligned} \frac{\partial D_i(q)}{\partial x} =& \frac{1}{D_i(q)} \Bigg((c^x - r^x)\left(\frac{\partial c^x}{\partial x} - 1 - \frac{\partial a}{\partial x}\cos\theta \right. \\ & \left. + \frac{\partial b}{\partial x}\sin\theta\right) + (c^y - r^y) \\ & \cdot \left(\frac{\partial c^y}{\partial x} - \frac{\partial a}{\partial x}\sin\theta - \frac{\partial b}{\partial x}\cos\theta\right)\Bigg) \\ =& \frac{1}{D_i(q)} \left\langle \begin{bmatrix} (c^x - r^x) \\ (c^y - r^y) \end{bmatrix}, \left(\begin{bmatrix} -1 \\ 0 \end{bmatrix} + \begin{bmatrix} \frac{\partial c^x}{\partial x} \\ \frac{\partial c^y}{\partial x} \end{bmatrix} \right. \right. \\ & \left. \left. - \begin{bmatrix} \frac{\partial a}{\partial x}\cos\theta - \frac{\partial b}{\partial x}\sin\theta \\ \frac{\partial a}{\partial x}\sin\theta + \frac{\partial b}{\partial x}\cos\theta \end{bmatrix} \right) \right\rangle \end{aligned}$$

Note that the vector $c - r$ is orthogonal to the tangent space of the boundary of the obstacle at c, as well as to the tangent space of the boundary of the robot at r. Note that $[\partial c^x/\partial x, \partial c^y/\partial x]^T$ is an element in the tangent space of the boundary of the obstacle and that $[\partial a/\partial x\cos\theta - \partial b/\partial x\sin\theta, \partial a/\partial x\sin\theta + \partial b/\partial x\cos\theta]^T$ is an element in the tangent space of the boundary of the robot. Therefore, the dot products of $c - r$ with both of these vectors is zero and thus we have

$$\frac{\partial D_i(q)}{\partial x} = \frac{1}{D_i(q)}(r^x - c^x). \tag{15}$$

Using similar analysis, we can easily conclude that

$$\frac{\partial D_i(q)}{\partial y} = \frac{1}{D_i(q)}(r^y - c^y). \tag{16}$$

Finally, consider $\partial D_i/\partial\theta$

$$\begin{aligned} \frac{\partial D_i(q)}{\partial \theta} = \frac{1}{D_i(q)} \Bigg(& (c^x - r^x)\left(\frac{\partial c^x}{\partial \theta} - \frac{\partial r^x}{\partial \theta}\right) \\ & + (c^y - r^y)\left(\frac{\partial c^y}{\partial \theta} - \frac{\partial r^y}{\partial \theta}\right)\Bigg). \end{aligned} \tag{17}$$

From (12),

$$\begin{aligned} \frac{\partial r^x}{\partial \theta} &= \frac{\partial a}{\partial \theta}\cos\theta - a\sin\theta - \frac{\partial b}{\partial \theta}\sin\theta - b\cos\theta \\ \frac{\partial r^y}{\partial \theta} &= \frac{\partial a}{\partial \theta}\sin\theta + a\cos\theta + \frac{\partial b}{\partial \theta}\cos\theta - b\sin\theta. \end{aligned} \tag{18}$$

Substitute the above into $\partial D_i(q)/\partial\theta$ in (17) to obtain

$$\begin{aligned}\frac{\partial D_i}{\partial\theta} =& \frac{1}{D_i(q)}\left((c^x-r^x)\left(\frac{\partial c^x}{\partial\theta}-\frac{\partial a}{\partial\theta}\cos\theta\right.\right.\\ &\left.+a\sin\theta+\frac{\partial b}{\partial\theta}\sin\theta+b\cos\theta\right)\\ &+(c^y-r^y)\left(\frac{\partial c^y}{\partial\theta}-\frac{\partial a}{\partial\theta}\sin\theta\right.\\ &\left.\left.-a\cos\theta-\frac{\partial b}{\partial\theta}\cos\theta+b\sin\theta\right)\right)\\ =&\frac{1}{D_i(q)}\left\langle\begin{bmatrix}(c^x-r^x)\\(c^y-r^y)\end{bmatrix},\left(\begin{bmatrix}a\sin\theta+b\cos\theta\\b\sin\theta-a\cos\theta\end{bmatrix}\right.\right.\\ &\left.\left.+\begin{bmatrix}\frac{\partial c^x}{\partial\theta}\\\frac{\partial c^y}{\partial\theta}\end{bmatrix}-\begin{bmatrix}\frac{\partial a}{\partial\theta}\cos\theta-\frac{\partial b}{\partial\theta}\sin\theta\\\frac{\partial a}{\partial\theta}\sin\theta+\frac{\partial b}{\partial\theta}\cos\theta\end{bmatrix}\right)\right\rangle\\ =&\frac{1}{D_i(q)}\left\langle\begin{bmatrix}(c^x-r^x)\\(c^y-r^y)\end{bmatrix},\begin{bmatrix}a\sin\theta+b\cos\theta\\b\sin\theta-a\cos\theta\end{bmatrix}\right\rangle\\ =&\frac{1}{D_i(q)}\begin{bmatrix}c^x-r^x\\c^y-r^y\end{bmatrix}^T\begin{bmatrix}0&1\\-1&0\end{bmatrix}\begin{bmatrix}\cos\theta&-\sin\theta\\\sin\theta&\cos\theta\end{bmatrix}\begin{bmatrix}a\\b\end{bmatrix}\\ =&\frac{1}{D_i(q)}\begin{bmatrix}c^x-r^x\\c^y-r^y\end{bmatrix}^T\begin{bmatrix}0&1\\-1&0\end{bmatrix}\begin{bmatrix}U^x\\U^y\end{bmatrix}\\ =&\frac{1}{D_i(q)}(c-r)\times U\\ =&U\times\nabla d_i(r)\end{aligned}$$

where U is described in world coordinates. That is, $U=\text{Rot}(\theta)[a,b]^T$. Therefore, the gradient is

$$\begin{bmatrix}\nabla d_i(r)\\U\times\nabla d_i(r)\end{bmatrix} \tag{19}$$

where $\nabla d_i(r)$ is a 3×1 vector that is the gradient of a single object distance function evaluated at r and U is as described above. Note that the cross product of two planar vectors is a scalar because the only meaningful component to the resulting cross product vector is the "z" component that sticks out of the plane spanned by the two co-planar vectors. The cross product of two-vectors S and T is often written as $S^T\begin{bmatrix}0&1\\-1&0\end{bmatrix}T$.

Appendix II
Incremental Construction of the Rod-GVG

Now that we have defined the rod-GVG, we use standard numerical construction techniques to construct it. Assume that the rod has accessed the rod-GVG. Let z_1 be the basis of the tangent space of the rod-GVG edge at configuration q and let z_1, z_2, z_3 be the basis of the tangent space of $SE(2)$ at q. That is, z_1, z_2, z_3 can be viewed as a coordinate frame whose origin is located at q. Let λ be a parameter which represents a displacement in the z_1 direction and let Y be the plane spanned by z_2 and z_3 (passing through the origin defined by q). This plane is termed the "normal plane" and is orthogonal to z_1, the tangent of the rod-GVG. Incremental construction of the rod-GVG edge is achieved by tracing the roots of the expression $G_{\text{rod}}(y;\lambda)=0$ for $y\in Y$ as the parameter λ varies:

$$G_{\text{rod}}(y;\lambda)=\begin{bmatrix}D_i(y;\lambda)-D_j(y;\lambda)\\D_i(y;\lambda)-D_k(y;\lambda)\end{bmatrix}. \tag{20}$$

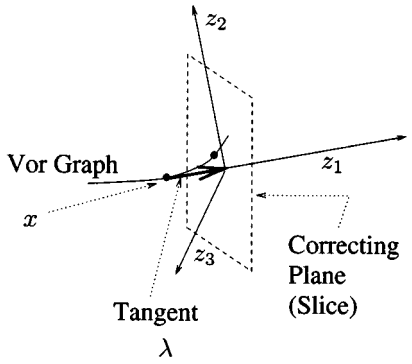

Fig. 20. Sketch of continuation method.

The function $G_{\text{rod}}(y;\lambda)$ assumes a zero value only on a rod-GVG edge. Hence, if the Jacobian of G_{rod}, which is

$$T_yG_{\text{rod}}(y;\lambda)=\begin{bmatrix}(\nabla D_i(y;\lambda)-\nabla D_j(y;\lambda))^T\\(\nabla D_i(y;\lambda)-\nabla D_k(y;\lambda))^T\end{bmatrix} \tag{21}$$

is surjective, then the implicit function theorem asserts that the roots of $G_{\text{rod}}(y;\lambda)$ locally define a rod-GVG edge as λ is varied. A rod-GVG edge is constructed by numerically tracing the roots of G. The explicit edge construction procedure has two steps: a predictor step and a corrector step. The predictor step moves the robot for a small distance along the tangent of the rod-GVG. The tangent direction is the null space of T_YG_{rod} [23]. This null space can be computed by

$$(\nabla D_i(y;\lambda)-\nabla D_j(y;\lambda))^T\times(\nabla D_i(y;\lambda)-\nabla D_k(y;\lambda))^T.$$

Since T_YG_{rod} comprises distance information, it can be readily computed with line of sight sensor information.

Typically, the prediction step takes the robot off of a rod-GVG edge, so a correction procedure is required to bring the robot back to the rod-GVG. If step size along the tangent is "small," then the graph will intersect a "correcting plane" (Fig. 20), which is a plane orthogonal to the tangent. The correction step finds the location where the rod-GVG intersects the correcting plane (Fig. 20) and is achieved via a iterative Newton's Method. If y^k and λ^k are the kth estimates of y and λ, the $k+1$st iteration is defined as

$$y^{k+1}=y^k-\left(T_yG_{\text{rod}}(y^k,\lambda^k)\right)^{-1}G_{\text{rod}}(y^k,\lambda^k) \tag{22}$$

where T_yG_{rod} is the Jacobian of G_{rod} restricted to the correcting plane evaluated at (y^k,λ^k).

Now, it needs to be shown that:

Proposition 4: The matrix T_yG_{rod} (restricted to the correcting plane) is invertible.

Proof: This proof is done in two steps. First, we know that $TG_{\text{rod}}(q)$ has rank two which is a simple consequence of transversality. Since $\mathcal{CF}_{ij}$ and $\mathcal{CF}_{jk}$ transversally intersect, then $T_q\mathcal{CF}_{ij}\neq\alpha T_qT_q\mathcal{CF}_{jk}$ where $\alpha\in\mathbb{R}$. Therefore, $\nabla(D_i(q)-D_j(q))\neq\alpha\nabla(D_j(q)-D_k(q))$ and hence the two rows of $TG_{\text{rod}}(q)$ are linearly independent of each other.

Second, we show that the $\text{rank}(TG_{\text{rod}}(q))=\text{rank}(T_yG_{\text{rod}}(y;\lambda))$. In fact, we show the two matrices are in fact equal. Once this is shown, then the proposition easily follows that $\text{rank}(TG_{\text{rod}}(q))=\text{rank}(T_yG_{\text{rod}}(y;\lambda))=2$, i.e., T_yG_{rod} is invertible.

Now, we will show that $\mathrm{rank}(TG_{\mathrm{rod}}(q)) = \mathrm{rank}(T_yG_{\mathrm{rod}}(y;\lambda))$. Let v is a unit vector that is parallel to z_1. That is,

$$v = \alpha((\nabla D_i(q) - \nabla D_j(q)) \times (\nabla D_i(q) - \nabla D_k(q))). \quad (23)$$

Then

$$\begin{aligned} v \cdot \nabla D_i(q) =& \alpha((\nabla D_i(q) - \nabla D_j(q)) \\ & \times (\nabla D_i(q) - \nabla D_k(q)) \cdot \nabla D_i(q) \\ =& \alpha(\nabla D_i(q) - \nabla D_j(q)) \\ & \cdot ((\nabla D_i(q) - \nabla D_k(q)) \times \nabla D_i(q)) \\ =& \alpha(\nabla D_i(q) - \nabla D_j(q)) \\ & \cdot (-\nabla D_k(q) \times \nabla D_i(q)). \end{aligned} \quad (24)$$

Also,

$$\begin{aligned} v \cdot \nabla D_k(q) =& \alpha((\nabla D_i(q) - \nabla D_j(q)) \\ & \times (\nabla D_i(q) - \nabla D_k(q)) \cdot \nabla D_k(q) \\ =& \alpha(\nabla D_i(q) - \nabla D_j(q)) \\ & \cdot ((\nabla D_i(q) - \nabla D_k(q)) \times \nabla D_k(q)) \\ =& \alpha(\nabla D_i(q) - \nabla D_j(q)) \\ & \cdot (\nabla D_i(q) \times \nabla D_k(q)) \\ =& \alpha(\nabla D_i(q) - \nabla D_j(q)) \\ & \cdot (-\nabla D_k(q) \times \nabla D_i(q)) \\ =& v \cdot \nabla D_i(q). \end{aligned} \quad (25)$$

Following similar steps, we can see that $v \cdot \nabla D_j(q) = v \cdot \nabla D_i(q)$. So $v \cdot \nabla D_i(q) = v \cdot \nabla D_j(q) = v \cdot \nabla D_k(q)$. That means the projections of $\nabla D_m, m = i, j, k$ in z_1 has same length. So,

$$\nabla D_i(q) - \nabla D_j(q) = [0 \quad \nabla_Y D_i(y) - \nabla_Y D_j(y)] \quad (26)$$

where ∇, ∇_y denote the gradient with respect to ambient and slice plane coordinates respectively.

So, in local coordinates z,

$$T_zG_{\mathrm{rod}}(y;\lambda) = \begin{pmatrix} (0 & \nabla_Y D_i(q) - \nabla_Y D_j(q))) \\ (0 & \nabla_Y D_i(q) - \nabla_Y D_k(q))) \end{pmatrix}. \quad (27)$$

So, $TG_{\mathrm{rod}} = [0 \quad T_YG_{\mathrm{rod}}] = [0 \quad \pi_Y TG_{\mathrm{rod}}]$.

Since T_yG_{rod} is invertible, (22) is well posed. Practically speaking, this result states that the numerical procedure defined by (22) will be robust for reasonable errors in robot position, sensor errors and numerical round off.

APPENDIX III

ROD-GVG EDGES ARE RETRACTS OF JUNCTION REGIONS

In this section, we prove Corollary 1 that demonstrates that each rod-GVG edge is a retract of a junction region. We do this by showing that the H function, or more specifically a perturbation of the H function, is a retraction.

Proof: Given two points x_1 and $x_2 \in \mathbb{R}^m$ with $|x_1 - x_2| = \lambda$ and a convex obstacle C, let c_1, c_2 be the closest points on the obstacle to x_1, x_2 respectively. Also, let d_1 and d_2 be their respective distance to the obstacle. Without loss of generality assume that $d_1 \leq d_2$. If $d_2 - d_1 > \lambda$, then $d_2 > d_1 + \lambda = |c_1 - x_1| + |x_1 - x_2| > |c_1 - x_2|$, which is a contradiction. Therefore,

$$|d_1 - d_2| \leq \lambda.$$

Also, for c_i's , let S_1 and S_2 be the spheres centered on x_1 and x_2 with radius d_1 and d_2, respectively and c_1c_2 be the line segment connecting c_1 and c_2. Consider a line segment whose end points are on each sphere such that the segment itself does not intersect the interior of either sphere. Since the centers of the sphere are λ apart, the length of this line segment is at most $\lambda = |x_1 - x_2|$. Therefore,

$$|c_1 - c_2| \leq \lambda. \quad (28)$$

Given two configuration of the rod q_1 and q_2, let q_m be the configuration such that $\Theta(q_m) = \Theta(q_1)$ and $P(q_m) = P(q_2)$. Then, $d(q_1, q_m) \leq d(q_1, q_2)$ and $d(q_2, q_m) \leq d(q_1, q_2)$. Then,

$$|r_1 - r_m| \leq |P(q_1) - P(q_m)| \leq d(q_1, q_m) \leq d(q_1, q_2)$$

where r_1, r_m are closest points on the rod to the obstacle at each configurations.

Now we consider q_m and q_2. Let c_ir_i be the vector defined by two points c_i and r_i and $PQ(q_i)$ be the vector defined by P and Q, the two end points of the rod at the configuration q_i. Given q_i, if $\angle(PQ(q_i))(c_ir_i) \neq \pi/2$, then r_i is on either P or Q. For those configurations, we can find a rod configuration q_i' such that $P(q_i) = P(q_i')$, $r_i = r_i'$ and $\angle(PQ(q_i'))(c_ir_i) = \pi/2$[4] (See Fig. 21) So, given q_m and q_2, let q_m' and q_2' be such configurations for each q_m and q_2. Then, $|r_2 - r_m| = |r_2' - r_m'|$, so, without loss of generality, we assume that $\angle(PQ(q_m))(c_mr_m) = \angle(PQ(q_2))(c_2r_2) = \pi/2$.

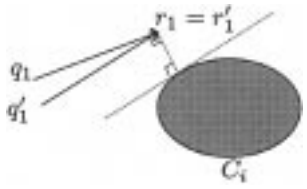

Fig. 21. When we rotate q_1 to q_1', the distance $D_i(q)$ and the closest point on the rod $r(q_1)$ does not change.

Let ρ_i be the radius of curvature of the wall of the obstacle at c_i and L be the length of the rod. Then

$$\begin{aligned} |r_m - r_2| \leq& M|(D(q_m) + \rho(q_m))\Theta(q_m) \\ & - (D(q_2) + \rho(q_2))\Theta(q_2)| \\ \leq& M(\max(D(q_m), D(q_2)) + \rho)d(q_m, q_2) \\ \leq& M(\max(D(q_m), D(q_2)) + \rho)d(q_1, q_2) \end{aligned}$$

for some constant M. Then, assuming that there is no 'flat' wall, $\rho < \rho_{\max}$ for some constant N and since the environment is bounded, i.e., $D(q) < D_{\max}$, for some $D_{\max}$. Thus,

$$|r_m - r_2| \leq K'd(q_1, q_2).$$

where $K' = (D_{\max} + \rho_{\max})$. Therefore, for any q_1 and q_2

$$\begin{aligned} |r_1 - r_2| \leq& |r_1 - r_m| + |r_m - r_2| \\ \leq& d(q_1, q_2) + K'd(q_1, q_2) = Kd(q_1, q_2) \end{aligned} \quad (29)$$

[4] $c_i' = c_1, r_i' = r_i$

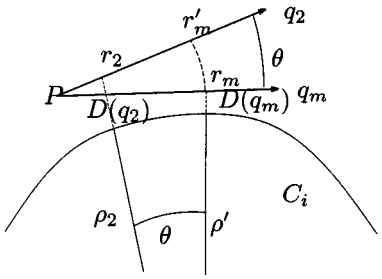

Fig. 22. Here, r_2 and r_m are the closest points on the rod at configurations q_2 and q_m each and r'_m is point on the rod at q_2 corresponding to r_m at q_m. Then, $|r_m - r_2| \leq |r_m - r'_m| + |r'_m - r_2| \leq L\theta + (\rho(q_2) + D_i(q_2))\theta$.

for some constant $K = (1 + K')$. Then, from (28) and (29),

$$|c_1 - c_2| \leq |r_1 - r_2| \leq Kd(q_1, q_2) \tag{30}$$

for some K.

Now, we want to show: $\dot{\underline{H}}(q,t)$ satisfies Lipschitz condition with respect to q in free space. First, for gradient ascent from the closest obstacle, $\dot{\underline{H}}(q,t) = \dot{\underline{H}}(q) = D_1(\underline{H}(q,t))\nabla(D_1(\underline{H}(q,t)))$, which is

$$\begin{aligned}\dot{\underline{H}}(q,t) =& D_1(\underline{H}(q,t))\nabla D_1(\underline{H}(q,t)) \\ =& \begin{bmatrix} \nabla d'_1(r(\underline{H}(q,t))) \\ U(\underline{H}(q,t)) \times \nabla d'_1(r(\underline{H}(q,t))) \end{bmatrix}\end{aligned}$$

where $\nabla d'_1(r) = (r - c)$ and $U(q) = r(q) - P(q)$. We want to show that

$$|\dot{\underline{H}}(q_1,t) - \dot{\underline{H}}(q_2,t)| < M|q_1 - q_2|$$

for some constant M (see the equation at the bottom of the page).

Since

$$\begin{aligned}|\nabla d'_1(r(\underline{H}(q_1,t)) - \nabla d'_1(r(\underline{H}(q_2,t)))| =& |(r_1 - c_1) - (r_2 - c_2)| \\ \leq& |r_1 - r_2| + |c_1 - c_2|\end{aligned}$$

from (29) and (30),

$$|\nabla d'_1(r(\underline{H}(q_1,t)) - \nabla d'_1(r(\underline{H}(q_2,t)))| \leq M_1 d(q_1, q_2)$$

for some constant M_1. Since,

$$|(r_1 - c_1) - (r_2 - c_2)| < (|r_1 - c_1| + |r_2 - c_2|) < 2d(q_1, q_2),$$

it follows that

$$|\nabla d_j(r_1) - \nabla d_j(r_2)| < 2d(q_1, q_2).$$

Also, for $U(q_1)$ and $U(q_2)$,

$$\begin{aligned}&|U(\underline{H}(q_1,t)) - U(\underline{H}(q_2,t))| \\ &\quad = |(r_1 - P(\underline{H}(q_1,t))) - (r_2 - P(\underline{H}(q_2,t)))| \\ &\quad = |(r_1 - r_2) - (P(\underline{H}(q_1,t)) - P(\underline{H}(q_2,t)))| \\ &\quad < |(r_1 - r_2)| + |P(\underline{H}(q_1,t)) - P(\underline{H}(q_2,t))|.\end{aligned}$$

Therefore,

$$|U(\underline{H}(q_1,t)) - U(\underline{H}(q_2,t))| \leq M_2 d(q_1, q_2)$$

for some constant M_2.

Hence, we have the equation shown at the bottom of the page for some constants M' and M''. Since $|U| \leq L$ and $|\nabla d'_2(r(\underline{H}(q_2,t)))| = |r(\underline{H}(q_2,t)) - c(\underline{H}(q_2,t))| \leq M'''$ for some M''' from the boundedness of the envitonment,

$$\begin{aligned}&|U(\underline{H}(q_1,t)) \times \nabla d'_1(r(\underline{H}(q_1,t))) \\ &\quad - U(\underline{H}(q_2,t)) \times \nabla d'_2(r(\underline{H}(q_2,t)))| \leq Nd(q_1, q_2)\end{aligned}$$

for some N.

So, $\dot{\underline{H}}(q,t)$ also satisfies Lipschitz condition, i.e.,

$$|\dot{\underline{H}}(q_1,t) - \dot{\underline{H}}(q_2,t)| < Md(q_1, q_2)$$

for some constant M for any q_1 and q_2. Therefore there exists $\underline{H}(q,t)$ which satisfies above condition and also continuous on t and the initial condition, i.e., q [24].

$$|\dot{\underline{H}}(q_1,t) - \dot{\underline{H}}(q_2,t)| = \begin{bmatrix} \nabla d'_1(r(\underline{H}(q_1,t))) - \nabla d'_1(r(\underline{H}(q_2,t))) \\ U(\underline{H}(q_1,t)) \times \nabla d'_1(r(\underline{H}(q_1,t))) - U(\underline{H}(q_2,t)) \times \nabla d'_1(r(\underline{H}(q_2,t))) \end{bmatrix}$$

$$\begin{aligned}&|U(\underline{H}(q_1,t)) \times \nabla d'_1(r(\underline{H}(q_1,t))) - U(\underline{H}(q_2,t)) \times \nabla d'_2(r(\underline{H}(q_2,t)))| \\ &= |U(\underline{H}(q_1,t)) \times \nabla d'_1(r(\underline{H}(q_1,t))) - U(\underline{H}(q_1,t)) \times \nabla d'_2(r(\underline{H}(q_2,t))) \\ &\qquad + U(\underline{H}(q_1,t)) \times \nabla d'_2(r(\underline{H}(q_2,t))) - U(\underline{H}(q_2,t)) \times \nabla d'_2(r(\underline{H}(q_2,t)))| \\ &= |U(\underline{H}(q_1,t)) \times (\nabla d'_1(r(\underline{H}(q_1,t))) - \nabla d'_2(r(\underline{H}(q_2,t)))) \\ &\qquad + (U(\underline{H}(q_1,t)) - U(\underline{H}(q_2,t))) \times \nabla d'_2(r(\underline{H}(q_2,t)))| \\ &\leq |U(\underline{H}(q_1,t)) \times (\nabla d'_1(r(\underline{H}(q_1,t))) - \nabla d'_2(r(\underline{H}(q_2,t))))| \\ &\qquad + |(U(\underline{H}(q_1,t)) - U(\underline{H}(q_2,t))) \times \nabla d'_2(r(\underline{H}(q_2,t)))| \\ &\leq |U(\underline{H}(q_1,t))||(\nabla d'_1(r(\underline{H}(q_1,t))) - \nabla d'_2(r(\underline{H}(q_2,t))))| \\ &\qquad + |(U(\underline{H}(q_1,t)) - U(\underline{H}(q_2,t)))||\nabla d'_2(r(\underline{H}(q_2,t)))| \\ &\leq M' d(q_1, q_2)|U(\underline{H}(q_1,t))| + M'' d(q_1, q_2)|\nabla d'_2(r(\underline{H}(q_2,t)))|\end{aligned}$$

For gradient ascent with double-, triple-equidistant, since $\dot{\underline{H}}(q,t) = \pi_T \nabla(D_1)$, or $\dot{\underline{H}}(q,t) = \nabla(D_1 - D_2)$ etc., it also satisfies the condition.

At this point, we could use $\underline{H}$ as our accessibility criterion and our retraction. From here we can conclude that the CF_{ijk} is a retraction of a junction region J_{ijk} using $\underline{H}$. In implementation we use H, which is defined as $H = \underline{H}(q,t)/D(\underline{H}(q,t))$.

ACKNOWLEDGMENT

The authors would also like to thank J. Burdick, A. Rizzi, M. Mason, S. Thrun, S. Hutchison, J.-P., B. Kuipers, T. Yata and I. Rekleitis for their encouragement and insight into this work. Finally, the authors would like to thank the anonymous reviewers for their careful and considerate comments toward this work.

REFERENCES

[1] J. F. Canny, *The Complexity of Robot Motion Planning*. Cambridge, MA: MIT Press, 1988.
[2] J. F. Canny and M. Lin, "An opportunistic global path planner," *Algorithmica*, vol. 10, pp. 102–120, 1993.
[3] J. C. Latombe, *Robot Motion Planning*. Boston, MA: Kluwer, 1991.
[4] E. Rimon and J. F. Canny, "Construction of C-space roadmaps using local sensory data—What should the sensors look for?," in *Proc. IEEE Int. Conf. on Robotics and Automation*, San Diego, CA, 1994, pp. 117–124.
[5] H. Choset and J. Burdick, "Sensor based motion planning: The hierarchical generalized voronoi graph," *Int. J. Robot. Res.*, vol. 19, no. 2, pp. 96–125, Feb. 2000.
[6] ——, "Sensor based motion planning: Incremental construction of the hierarchical generalized voronoi graph," *Int. J. Robot. Res.*, vol. 19, no. 2, pp. 126–148, Feb. 2000.
[7] N. S. V. Rao, S. Kareti, W. Shi, and S. S. Iyenagar, "Robot navigation in unknown terrains: Introductory survey of nonheuristic algorithms," *Oak Ridge National Laboratory Tech. Rep.*, vol. ORNL/TM-12 410, pp. 1–58, July 1993.
[8] V. Lumelsky and A. Stepanov, "Path planning strategies for point mobile automaton moving amidst unknown obstacles of arbitrary shape," *Algorithmica*, vol. 2, pp. 403–430, 1987.
[9] F. Aurenhammer, "Voronoi diagrams—A survey of a fundamental geometric structure," *ACM Computing Surveys*, vol. 23, pp. 345–405, 1991.
[10] H. Choset, "Nonsmooth analysis, convex analysis and their applications to motion planning," *Int. J. Comp. Geom. Applicat.*, 1998.
[11] P. F. Rowat, "Representing the Spatial Experience and Solving Spatial Problems in a Simulated Robot Environment," Ph. D. , University of British Columbia, 1979.
[12] C. Ó'Dúnlaing and C. K. Yap, "A "Retraction" method for planning the motion of a disc," *Algorithmica*, vol. 6, pp. 104–111, 1985.
[13] C. Ó'Dúnlaing, M. Sharir, and C. K. Yap, "Generalized Voronoi diagrams for moving a ladder. I: Topological analysis," *Commun. Pure Appl. Math.*, vol. 39, pp. 423–483, 1986.
[14] J. Cox and C. K. Yap, "On-line motion planning: Case of a planar rod," *Ann. Math. Artif. Intell.*, vol. 3, pp. 1–20, 1991.
[15] J. T. Schwartz and C. K. Yap, *Advances in Robotics: Algorithmic and Geometric Apsects of Robotics*, J. T. Schwartz and C. K. Yap, Eds, NJ: Lawrence Erlbaum Associates, 1987, vol. 1.
[16] O. Takahashi and R. J. Schilling, "Motion planning using generalized voronoi diagrams," *IEEE Trans. Robot. Automat.*, vol. 5, pp. 143–150, Apr. 1989.
[17] N. S. V. Rao, N. Stolzfus, and S. S. Iyengar, "A retraction method for learned navigation in unknown terrains for a circular robot," *IEEE Trans. Robot. Automat.*, vol. 7, pp. 699–707, Oct. 1991.
[18] H. Choset, W. Henning, F. Hickman, R. Knepper, D. Jackson, S. Walker, J. Flasher, and A. Alford. (1999) Software to Generate the GVD and HGVG. [Online]. Available: http://voronoi.sbp.ri.cmu.edu/
[19] V. Guillemin, *Differential Topology*, A. Pollack, Ed. Englewood Cliffs, NJ: Prentice-Hall, 1974.
[20] F. H. Clarke, *Optimization and Nonsmooth Analysis*. Philadelphia, PA: SIAM, 1990.
[21] F. C. Park, "Distance metrics on the rigid-body motions with applications to mechanism desgin," *ASME J. Mech. Design*, 1995.
[22] T. Lozano-Perez and M. A. Wesley, "An algorithm for planning collision-free paths among polyhedral obstacles," *Commun. ACM*, vol. 22, no. 10, pp. 560–570, 1979.
[23] J. A. Thorpe, *Elementary Topics in Differential Geometry*. Berlin, Germany: Springer-Verlag, 1985.
[24] B. Louis, *Differential and Difference Equations*. New York: Wiley, 1966.

Howie Choset (S'93–M'96) is an Associate Professor of Mechanical Engineering, Robotics, Electrical and Computer Engineering at Carnegie Mellon University, Pittsburgh, PA, where he conducts research in motion planning and design of serpentine mechanisms, coverage path planning for de-mining and painting, mobile robot sensor based exploration of unknown spaces, distributed manipulation with macroscopic arrays and education with robotics. He directs the Undergraduate Robotics Minor at Carnegie Mellon and teaches an overview course on Robotics. Recently, he developed a series of Lego Labs to complement the course work and will be implementing these labs in the Fall.

Prof. Choset received the National Science Foundation Career Award in 1997 to continue the work in the underlying fundamentals of roadmaps for arbitrarily shaped objects; the long-term goal of this work is to define roadmaps for highly articulated robots. He also recently received support from the Office of Naval Research through its Young Investigator Program to develop strategies to search for land and sea mines and to construct a land-mine-search robot. He co-chairs the IEEE Technical Committee on Mobile Robots and co-chairs the SPIE Mobile Robots Conference each year. In 1999, he co-chaired the Field and Service Robotics conference and has co-organized a workshop on distributed manipulation; he co-edited a book on the subject.

Ji Yeong Lee received the B.S. and M.S. degrees in mechanical engineering from Seoul National University, Seoul, Korea, in 1991 and 1993, respectively. He is currently working toward the Ph.D. degree at Carnegie Mellon University, Pittsburgh, PA, under the advisement of Prof. Howie Choset.

He worked at Automation Research Institute of Samsung Electronics, Korea, from 1993 to 1998. His research interest is the motion planning of the rod-shaped robots in sensor-based way.